Original Article

Immune profile analysis of peripheral blood and tumors of lung cancer patients treated with immune checkpoint inhibitors

Yoshinobu Ichiki[1,2], Takashi Fukuyama[3], Mari Ueno[4], Yoshiro Kanasaki[1], Hidenori Goto[1], Mai Takahashi[5], Shuji Mikami[4], Noritada Kobayashi[3], Kozo Nakanishi[1], Shinichi Hayashi[5], Tsuyoshi Ishida[4]

[1]Department of General Thoracic Surgery, National Hospital Organization, Saitama Hospital, Wako, Japan; [2]Second Department of Surgery, University of Occupational and Environmental Health, School of Medicine, Kitakyushu, Japan; [3]Division of Biomedical Research, Kitasato University Medical Center, Kitamoto, Japan; [4]Department of Diagnostic Pathology, National Hospital Organization, Saitama Hospital, Wako, Japan; [5]Department of Respiratory Medicine, National Hospital Organization, Saitama Hospital, Wako, Japan

Contributions: (I) Conception and design: Y Ichiki, T Fukuyama; (II) Administrative support: Y Ichiki, T Fukuyama, M Ueno; (III) Provision of study materials or patients: Y Ichiki; (IV) Collection and assembly of data: Y Ichiki, Y Kanasaki, H Goto, K Nakanishi; (V) Data analysis and interpretation: Y Ichiki, M Ueno, S Mikami, T Ishida; (VI) Manuscript writing: All authors; (VII) Final approval of manuscript: All authors.

Correspondence to: Yoshinobu Ichiki, MD, PhD. Department of General Thoracic Surgery, National Hospital Organization Saitama Hospital, 2-1 Suwa, Wako 351-0102, Japan. Email: y-ichiki@med.uoeh-u.ac.jp.

Background: Immune checkpoint inhibitors (ICIs) have become central to lung cancer drug therapy, and establishing biomarkers that can predict effects and adverse events (AEs) is awaited. We prospectively analyzed the association between the immune-related molecular expression in peripheral blood mononuclear cells (PBMCs) and lung cancer tissues, and the effects of ICI monotherapy.

Methods: Twenty-one patients with advanced non-small cell lung cancer (NSCLC) who received ICI monotherapy were included. Changes in the expression of immune-related molecules in PBMCs before and after the administration of ICI were analyzed by flow cytometry. The major histocompatibility complex (MHC) class I and programmed cell death-ligand 1 (PD-L1) expression of cancer cells, and the PD-L1, CD8 and CD103 expression of tumor infiltrating immune cells in lung cancer tissue before the administration of ICI were confirmed by immunohistochemistry (IHC).

Results: Twenty-one patients were investigated, including 11 adenocarcinoma and 10 squamous cell carcinoma cases. Anti-programmed cell death protein-1 (PD-1) antibody (n=18) and anti-PD-L1 antibody (n=3) were administered. The clinical responses were graded as follows: complete response (CR) (n=1), partial response (PR) (n=7), stable disease (SD) (n=10) and progressive disease (PD) (n=3). Among immune-related molecules expressed in PBMCs, the $CD103^+$ $CD39^+$ $CD8^+$ T cell change after administration closely correlated with the clinical response. In the univariate analyses of the factors associated with progression-free survival (PFS), $CD103^+$ $CD39^+$ $CD8^+$ cell change after administration was identified as a significant prognostic factor, while the $CD103^+$ $CD39^+$ $CD8^+$ cell change after administration and Brinkman index were independent prognostic factors in a multivariate analysis of the factors associated with PFS.

Conclusions: The $CD103^+$ $CD39^+$ $CD8^+$ cell change after administration may predict the efficacy of ICIs.

Keywords: Lung cancer; immune checkpoint inhibitor (ICI); CD103; PD-1; tumor immunology

Submitted Jun 04, 2022. Accepted for publication Oct 13, 2022.
doi: 10.21037/tlcr-22-421
View this article at: https://dx.doi.org/10.21037/tlcr-22-421

Introduction

Immune checkpoint inhibitors (ICIs) were applied to the treatment of non-small cell lung cancer (NSCLC) and brought a paradigm shift resulting in an improved prognosis for NSCLC (1-4). However, there are still many unclear points about the mechanism of effect and predictors of the effect of ICIs. In clinical practice, tumor programmed cell death-ligand 1 (PD-L1) expression is an excellent biomarker, but it is often found that it does not correlate with clinical efficacy. In recent years, the combination therapy with ICIs and anticancer drugs for NSCLC have brought excellent effects and the numbers of patients receiving ICI monotherapy have decreased which have delayed investigations to identify the specific mechanism underlying the effect of ICIs on the host immune response is postponed.

Programmed cell death protein-1 (PD-1) is expressed on the cell surface of T lymphocytes and regulates hyper-autoimmune responses. Programmed cell death-ligand PD-L1, an immune-modulating ligand of PD-1, is expressed on not only cancer cells but also antigen-presenting cells. ICIs block the immune checkpoint molecules expressed on cancer cells or immune cells: thus, blocking inhibitory signals from ligands and prolonging T lymphocyte activation (5). The expression of PD-L1 on cancer cells in tissue specimens was related to the efficacy of anti-PD-1 therapy (6). The PD-L1 expression on cancer cells was recently reported to predict the effect of anti-PD-1 therapy in clinical practice: however, it is not a complete biomarker for predicting the effect of ICI therapy.

Cancer progression causes the exhaustion of lymphocytes (7,8). The exhaustion of lymphocytes induces the attenuation of the effector function and memory recall, metabolic dysregulation, and homeostatic self-renewal (9). In addition, exhausted lymphocytes express PD-1, cytotoxic T lymphocyte-related protein-4 (CTLA-4), and T cell immunoreceptor with Ig and ITIM domains (TIGIT), which are inhibitory receptors, and suppress their effector function (10).

If an accurate predictor could be identified in peripheral blood samples, it would provide a convenient potential biomarker that can be obtained safely and quickly (11,12). Therefore, we analyzed the relationship of immune-related molecular changes in peripheral blood mononuclear cells (PBMCs) caused by the administration of ICIs.

Pre- and post-treated PBMCs from lung cancer patients who received ICI monotherapy were analyzed using antibodies specific to coinhibitory molecules [PD-1, CTLA-4, LAG-3, TIM-3, TIGIT (9)] and costimulatory molecules [OX40 and 4-1BB (13)] to confirm the expression intensity and clinical response to ICI therapy by performing flow cytometry. In addition, immunosuppressive cells, such as effector regulatory T cells (eTreg cells) (14) and myeloid-derived suppressor cells (MDSCs) (15) and tumor specific T lymphocytes such as $CD103^+$ $CD39^+$ $CD8^+$ cells (16) were also analyzed. We investigated the relationship between the obtained molecular profile and therapeutic effects and adverse events (AEs).

We then confirmed whether the changes in the immune molecular profile in PBMCs were also related to the tumor microenvironment by using immunohistochemistry (IHC). In lung cancer biopsy tissues and surgical specimens before ICI monotherapy, the expression of the immunoregulatory molecules PD-L1, immune promoting molecules [e.g., major histocompatibility complex (MHC) class I], expression and tumor infiltrating lymphocytes (TILs) with the expression of CD8 or CD103 were analyzed using IHC to investigate the relationship between the obtained immune molecular profile and therapeutic effects and AEs. We present the following article in accordance with the REMARK reporting checklist (available at https://tlcr.amegroups.com/article/view/10.21037/tlcr-22-421/rc).

Methods

Patients and samples

From August 2019 to February 2022, 21 patients with advanced or recurrent NSCLC who received ICI monotherapy were included, regardless of the treatment line. The pathological and clinical stage (p-stage and c-stage) was determined based on the current tumor, node, metastasis (TNM) classification (17). The clinical response was evaluated by the following Response Evaluation Criteria in Solid Tumors version 1.1 (RECIST v 1.1.) (18). PBMCs of the patients were collected and cryopreserved before ICI therapy, and at 4 and 8 weeks after the start of ICI therapy (*Figure 1*). PBMCs were immediately isolated from blood samples using lymphocyte separation medium (cat. no. 0850494; MP Biomedicals, Irvine, USA). The relationship between changes in the immune molecular profile of PBMCs after ICI therapy and clinical response was also analyzed by flow cytometry (*Figure 1*).

Next, MHC class I, PD-L1 expression, CD8- and CD103-positive lymphocyte infiltration in lung cancer tissue before ICI therapy were analyzed to confirm whether the obtained changes in the immune molecular profile of

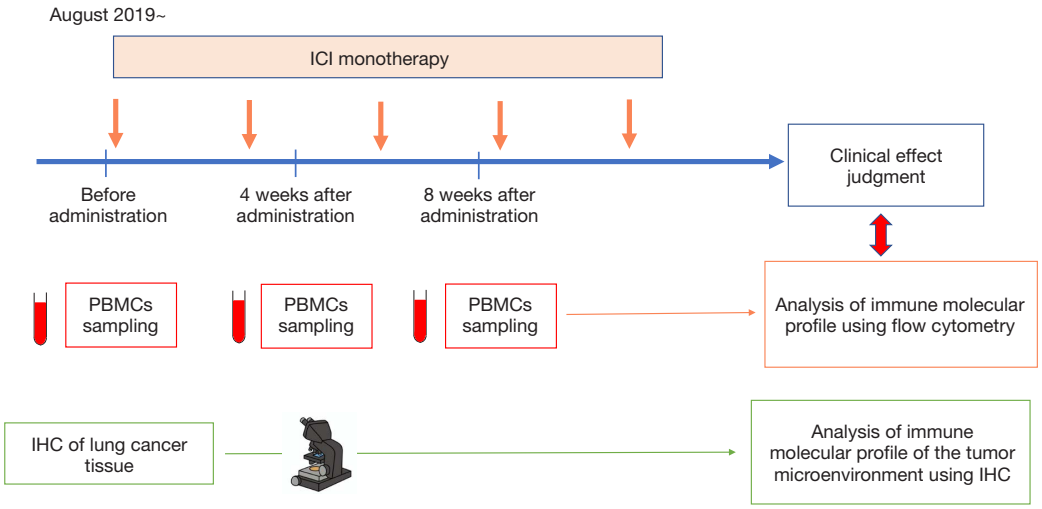

Figure 1 Twenty-one NSCLC patients who received ICI monotherapy were enrolled. PBMCs were collected from the patients and cryopreserved before ICI therapy, and at 4 and 8 weeks after ICI therapy. The relationship between changes in the immune-related molecules of PBMCs after ICI therapy and the clinical response was also analyzed by flow cytometry. Then serial sections from paraffin-embedded tumors, which were obtained before ICI monotherapy, were stained with anti-CD8, anti-CD103, anti-PD-L1, and anti-MHC class I antibodies. ICI, immune checkpoint inhibitor; PBMCs, peripheral blood mononuclear cells; IHC, immunohistochemistry; NSCLC, non-small cell lung cancer; PD-L1, programmed cell death-ligand 1; MHC, major histocompatibility complex.

PBMCs were also related with tumor microenvironment by IHC. We prospectively analyzed the relationship between clinicopathological factors, including the immune molecular profile of PBMCs and the tumor microenvironment, and the effect of ICI monotherapy.

This study was conducted in accordance with the Declaration of Helsinki (as revised in 2013). The study protocol was approved by the Saitama Hospital Ethics Committee (No. R2019-02). All participants gave informed consent before participation.

Flowcytometry of PBMCs

The following fluorescent-labeled antibodies were used: fluorescein isothiocyanate (FITC) anti-TIM-3 (F38-2E2) (cat. no. 345021; BioLegnd, San Diego, USA), FITC anti-OX40 (Ber-ACT35) (cat. no. 350006; BioLegnd), FITC anti-4-1BB [4B4 (4B4-1)] (cat. no. ab93520; Abcam, Cambridge, UK), FITC anti-CD103 (Ber-ACT8) (cat. no. 350203; BioLegnd), FITC anti-TIGIT (MBSA43) (cat. no. 11-9500-42; Invitrogen, Carlsbad, USA), Alexa Flour 488 anti-CD45RA (HI100) (cat. no. 304114; BioLegnd), FITC anti-CD33 (WM53) (cat. no. MCA1271; BIO RAD, Hercules, CA, USA), Alexa Flour 488 anti-GITR (108-17) (cat. no. 371209; BioLegnd), FITC anti-TCRab (LIP263) (cat. no. 306705; BioLegnd), PE-CF594 anti-LAG3 (T47-530) (cat. no. 12-2239-41; Invitrogen), PE anti-CTLA-4 (BNI3) (cat. no. IP-785-T025; Tonbo bioscience, San Diego, USA), PE anti-CD39 (A1) (cat. no. 328207; BioLegnd), PE anti-CD56 (HCD56) (cat. no. 318305; BioLegnd), PE anti-CD45RO (UCHL1) (cat. no. 304205; BioLegnd), PE anti-human leukocyte antigen-DR isotype (HLA-DR) (L243) (cat. no. 307605; BioLegnd), PE anti-CD25 (BC96) (cat. no. 302605; BioLegnd), PE anti-Ki-67 (Ki-67) (cat. no. 350503; BioLegnd), PE-eFluor 610 anti-PD-1 (eBioJ105) (cat. no. 61-2799-42; Invitrogen), PE anti-CD62L (DREG-56) (cat. no. 12-0929-41; Thermo Fisher Scientific, Waltham, USA), PE-eFluor 610 anti-CD11b (M1/70) (cat. no. 61-0112-80; Thermo Fisher Scientific), PE-Texas-Red anti-Granzyme B (GB11) (cat. no.#GRB17; Invitrogen), PE/Cyanine5 anti-CD4 (OKT-4) (cat. no. 317412; BioLegnd), PerCP-Cy 5.5 anti-CD14 (M5E2) (cat. no. 561116; BD), PE/Cyanine 7 anti-CD8 (HIT8a) (cat. no. 300914; BioLegnd), PE/Cyanine7 anti-CCR7 (G043H7) (cat. no. 353225; BioLegnd), PE-Cy7 anti-CD15 (HI98) (cat. no. 560827; BioLegnd), PE-Cyanine7 anti-foxp3 (PCH101) (cat. no. 25-4776-42; Invitrogen) (*Table 1*).

Cell surface staining was performed in PBS. Intracellular staining was performed using the Fix/Perm kit from eBioscience, San Diego, USA according to the

Table 1 Flow cytometry of PBMCs

Flow cytometer	FC500 (Beckman Coulter)				
	FL1	FL2	FL3	FL4	FL5
1	TIM3	LAG3	PD-1	CD4	CD8
2	OX40	LAG3	PD-1	CD4	CD8
3	4-1BB	CTLA-4	PD-1	CD4	CD8
4	CD103	CD39	PD-1	CD4	CD8
5	TIGIT	CD56	PD-1	CD4	CD8
6	CD45RA	CD45RO	CD62L	CD4	CCR7
7	CD33	HLADR	CD11b	CD14	CD15
8	CD45RA	CD25	PD-1	CD4	Foxp3*
9	CD45RA	Ki67*	PD-1	None	Foxp3*
10	GITR	Ki67*	PD-1	CD4	CD8
11	4-1BB	Ki67*	Granzyme*	CD4	CD8
12	TCRαβ	Ki67*	Granzyme*	CD4	CD8

*, intracellular molecules. PBMCs, peripheral blood mononuclear cells; PD-1, programmed cell death protein-1; CTLA-4, cytotoxic T lymphocyte-related protein-4; TIGIT, T cell immunoreceptor with Ig and ITIM domains; TCR, T cell receptor.

manufacturer's instructions. Intracellular molecule staining was performed using the IntraPrep Permeabilization Reagent kit from Beckman Coulter (Fullerton, USA) according to the manufacturer's instructions. Stained cells were detected using a CYTOMICS FC 500 flow cytometer (cat. no. B27017, Beckman Coulter). Data were analyzed using the FlowJo software program (Treestar).

IHC using pretreatment lung cancer tissue specimens

Hematoxylin and eosin (HE)-stained specimens of excised sections were used to evaluate TILs. TILs were evaluated according to the method of a previous report (19). (I) Calculate the ratio of the area where immune cells (lymphocytes, plasma cells) exist to the whole including not only hot spots but also stromal tissues, and use it as the median value. (II) Exclude lymphoid follicles (tertiary lymphatic structure) with granulocytes and germinal centers. (III) Exclude lymphocyte colonies away from the infiltrate of the cancer, even without germinal centers. Exclude necrosis and artifacts. (IV) Exclude lymphocyte infiltration away from the stroma close to the tumor even at the tumor border. (V) Exclude lymphocyte infiltration in normal lung tissue, even in close proximity to the tumor. (VI) Exclude lymphocytes that have infiltrated into the tumor tissue.

Serial sections from paraffin-embedded tumors were stained with anti-CD8 (SP57) (Roche diagnostics, Basel, Switzerland), anti-CD103 {EPR4166[2]} (Abcam), anti-PD-L1 (SP263) (Roche diagnostics), and anti-MHC class I [HLA-A,B,C] (EMR8-5.1) (MBL, Tokyo, Japan). The Benchmark XT autostainer (Ventana Medical System, Tucson, AZ, USA) was used for IHC. For the evaluation of $CD8^+$ and $CD103^+$ lymphocytes, two pathologists used the same method that was applied for TILs to count the proportion of the tumor stroma area in where IHC-positive TILs were present. The analysis was then performed using the median value. Regarding the MHC class I expression, the ratio of cancer cells expressing MHC class I among viable cancer cells was used. The ratio of the area of IHC-positive cancer cells to the total area of viable cancer cells was calculated to evaluate the PD-L1 expression in cancer cells. For the analysis of the PD-L1 expression in immune cells, the ratio of the area of IHC-positive immune cells to the total area of viable immune cells was also calculated (*Figure 1*).

Statistical analyses

Survival was analyzed using the Kaplan-Meier method. Log-rank tests were applied in univariate analyses and a Cox proportional hazards model was applied as a multivariate analysis.

A receiver operating characteristic (ROC) curve analysis

Table 2 The patient characteristics

Characteristics	Values
Age, years, median [range]	73.5 [56–82]
Sex, n [%]	
Male	17 [81]
Female	4 [19]
PS, n [%]	
0	15 [71]
1	5 [24]
2	1 [5]
Brinkman index, median [range]	1,080 [380–2,680]
Histologic type, n [%]	
Adenocarcinoma	11 [52]
Squamous cell carcinoma	10 [48]
c-stage or postoperative recurrence, n [%]	
Stage III	5 [24]
Stage IV	4 [19]
Recurrence	12 [57]
ICI, n [%]	
Pembrolizumab	17 [81]
Nivolumab	1 [5]
Atezolizumab	2 [9]
Durvalumab	1 [5]
Line, n [%]	
1st	14 [67]
1.5th	1 [5]
2nd	6 [28]
TCs % (SP263), n [%]	
<1	7 [33]
1–49	6 [29]
≥50	7 [33]
Not available	1 [5]
Response, n [%]	
CR + PR	8 [38]
SD + PD	13 [62]
irAE, n [%]	
Positive	9 [43]
Negative	12 [57]
NLR, %, median [range]	4.11 [0.84–12.29]
LDH, %, median [range]	170.5 [130–330]
CRP, %, median [range]	0.61 [0.05–10.22]
PET, SUV, median [range]	10.0 [3–27]

PS, performance status; c-stage, clinical stage; ICI, immune checkpoint inhibitor; TCs, tumor cells; CR, complete response; PR, partial response; SD, stable disease; PD, progressive disease; irAE, immune-related adverse effect; NLR, neutrophil-to-lymphocyte ratio; LDH, lactate dehydrogenase; CRP, C-reactive protein; PET, positron emission tomography; SUV, standardized uptake value.

was used to determine the cut-off values of the obtained clinicopathological data. The molecular expression was compared using *t*-tests, Pearson's product-moment correlation coefficient, repeated measures analysis of variance (ANOVA), and one-way ANOVA. All P values were two-sided. P values of <0.05 were considered to indicate statistical significance. Statistical analyses were performed using EZR (Saitama Medical Center, Jichi Medical University, Saitama, Japan), which is a graphical user interface for R (The R Foundation for Statistical Computing, Vienna, Austria). More precisely, it is a modified version of R commander designed to add statistical functions frequently used in biostatistics (20).

Results

Patient characteristics

The patients' characteristics are shown in *Table 2*. Twenty-one patients (male, n=17; female, n=4) were included in the present study. The median age of the enrolled patients was 73.5 years (range, 56–82 years). There were 11 cases of adenocarcinoma and 10 cases of squamous cell carcinoma. Anti-PD-1 antibody (n=18) and anti-PD-L1 antibody (n=3) were administered as ICIs. The performance status (PS) was classified as follows, PS 0 (n=15), PS 1 (n=5) and PS 2 (n=1). The median observation period was 220 days (range, 29–918 days). The clinical response to ICI therapy was classified as follows: complete response (CR; n=1), partial response (PR; n=7), stable disease (SD; n=10) and progressive disease (PD; n=3).

Analysis of the immune molecular profile of PBMC using flow cytometry

The expression of various immune-related molecules, as

shown in *Table 1*, was analyzed by flow cytometry, to search for molecules related to the clinical response. $CD103^+$ $CD39^+$ $CD8^+$ cells showed the strongest relationship with the response to ICI therapy (*Figure 2A*). When the patients were classified into CR + PR, SD, and PD groups and the transition of $CD103^+$ $CD39^+$ $CD8^+$ cells after treatment was compared, a significant difference was observed. PD-1^+ $CD8^+$ cells, eTreg cells, and MDSCs were also presented as representative immune cells, but no significant correlation was found in any of the groups (*Figure 2B-2D*).

Next, we analyzed whether the increase in $CD103^+$ $CD39^+$ $CD8^+$ cells after ICI therapy was associated with the prognosis. From the ROC curve, the value with the highest sensitivity and specificity was set as the cut-off value (*Figure 3A*). The increase in $CD103^+$ $CD39^+$ $CD8^+$ cells after administration significantly prolonged PFS. There was no significant difference in cancer-specific survival (*Figure 3B*).

The pretreatment $CD103^+$ $CD39^+$ $CD8^+$ cell count was also analyzed to show if it was correlated with the therapeutic effect. There was a significant difference in the relationship between the pretreatment $CD103^+$ $CD39^+$ $CD8^+$ cell count and the clinical response to ICI therapy (*Figure 4A*). However, the pretreatment $CD103^+$ $CD39^+$ $CD8^+$ cell count did not prolong either PFS or cancer-specific survival (*Figure 4B*).

Analysis of the immune molecular profile of lung cancer tissues using IHC

Since we had collected lung cancer tissues before ICI therapy in each case, we performed IHC using these samples and analyzed the expression of immune-related molecules, including the CD103 molecule, in the lung cancer tissues. The infiltration of $CD103^+$ cells in the tumor before treatment (IHC data) was significantly correlated with the increase of $CD103^+$ $CD39^+$ $CD8^+$ cells in PBMCs after ICI therapy, but was not significantly correlated with the pretreatment $CD103^+$ $CD39^+$ $CD8^+$ cell count in PBMCs (*Figure 4C*).

Prognosis analysis

The effects of clinicopathological factors, including typical immune cells (e.g., $CD103^+$ $CD39^+$ $CD8^+$ cells) in peripheral blood on the prognosis were analyzed. The cut-off value was calculated from the ROC curve (*Table 3*). A univariate analysis of clinicopathological factors for progression-free survival (PFS) showed that the $CD103^+$ $CD39^+$ $CD8^+$ cell change after ICI therapy was a significant prognostic factor. The multivariate analysis of clinicopathological factors associated with PFS showed that the $CD103^+$ $CD39^+$ $CD8^+$ cell change after ICI therapy and the Brinkman index were independent prognostic factors (*Table 4*). The univariate analysis of clinicopathological factors for cancer-specific survival showed that the Brinkman index was the only significant prognostic factor. A multivariate analysis of clinicopathological factors for cancer-specific survival showed no independent prognostic factors (*Table 5*).

Analysis of association with AE

Immune-related AEs were observed in 9 of 21 cases. We analyzed whether the immune-related cells in PBMCs including the $CD103^+$ $CD39^+$ $CD8^+$ cells detected in this study were correlated with AEs. The correlation of immune cells, such as the pretreatment $CD103^+$ $CD39^+$ $CD8^+$ cell, PD-1^+ $CD8^+$ cells, eTreg cells and MDSC counts and the change of $CD103^+$ $CD39^+$ $CD8^+$ cells after ICI therapy, with AEs was investigated but no related factors were found (*Figure 4D*).

Discussion

In this study, we searched for immune molecules related to the effects of ICI in 21 lung cancer patients who received ICI therapy. Our findings suggested that the change of $CD103^+$ $CD39^+$ $CD8^+$ cells in PBMCs after administration may significantly contribute to a favorable clinical response and improved PFS. The change in $CD103^+$ $CD39^+$ $CD8^+$ cells after administration may be a predictor of ICI efficacy. The relationship between the effects of ICIs and other immune cells, including immunosuppressive cells, such as eTreg cells and MDSCs was also investigated, but no significant factors were found. CD103, which is known as integrin αEβ7, is expressed on dendritic cells in the gut and T cells found in peripheral tissues, which are known as tissue resident memory T cells (21-23). CD103 interacts with the E-cadherin expressed in epithelial cells and mediates cell adhesion, migration, and cell lymphocyte homing (24). The CD103 expression was upregulated by TGF-b (25).

We previously focused on and analyzed the expression of immunological molecules in the microenvironment of primary tumors and regional lymph nodes using resected sections from 50 patients with squamous cell carcinoma of the lung. The expression of MHC class I and PD-L1

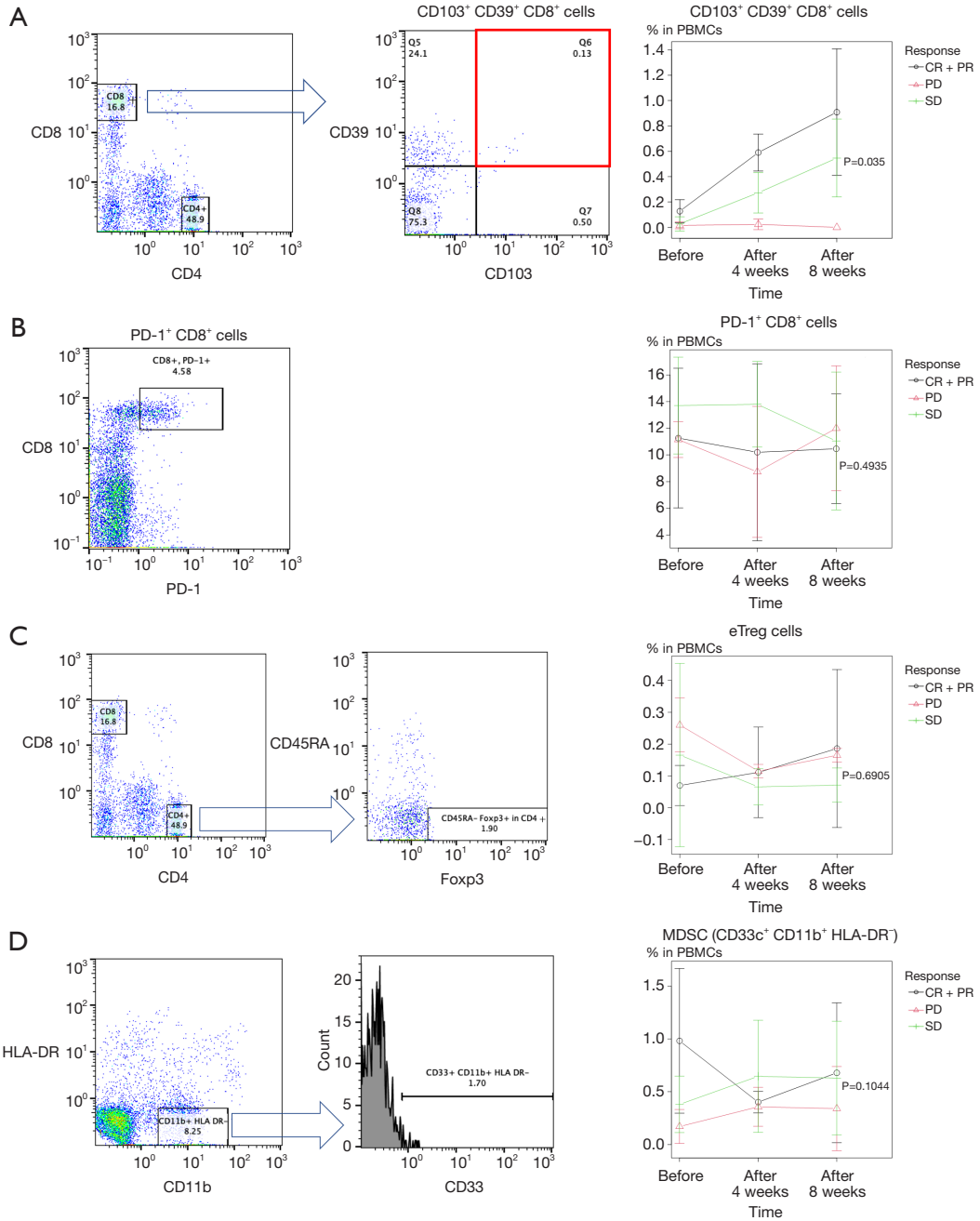

Figure 2 Analysis of the immune molecular profiles of PBMCs using flow cytometry was shown. (A) The characteristics of CD103$^+$ CD39$^+$ CD8$^+$ cells are shown. CD8$^+$ cells were gated from, PBMCs and CD103$^+$ CD39$^+$ was detected to obtain CD103$^+$ CD39$^+$ CD8$^+$ cells (the left and middle figures). The relationship between the change of CD103$^+$ CD39$^+$ CD8$^+$ cells after the administration of ICI therapy and the clinical response analyzed by a repeated measures ANOVA is shown in the right figure. (B) As one of the representative populations, PD-1$^+$ and CD8$^+$ populations were detected from PBMCs, and the relationship to the clinical response is shown. (C) The characteristics of eTreg cells are shown as one of the representative populations. CD4$^+$ cells were gated from PBMCs, and CD45RA$^-$ and Foxp3$^+$ were detected and regarded as eTreg cells (left and middle figures). The right figure shows the relationship between the change of eTreg cells after the administration and the clinical response. (D) As one of the representative populations, the characteristics of MDSCs are shown (the left and middle figures). The right figure shows the relationship between the change of MDSCs after administration and the clinical response. PBMCs, peripheral blood mononuclear cells; CR, complete response; PR, partial response; PD, progressive disease; SD, stable disease; PD-1, programmed cell death protein-1; eTreg cells, effector regulatory T cells; MDSC, myeloid-derived suppressor cell; HLA-DR, human leukocyte antigen-DR isotype; ANOVA, analysis of variance.

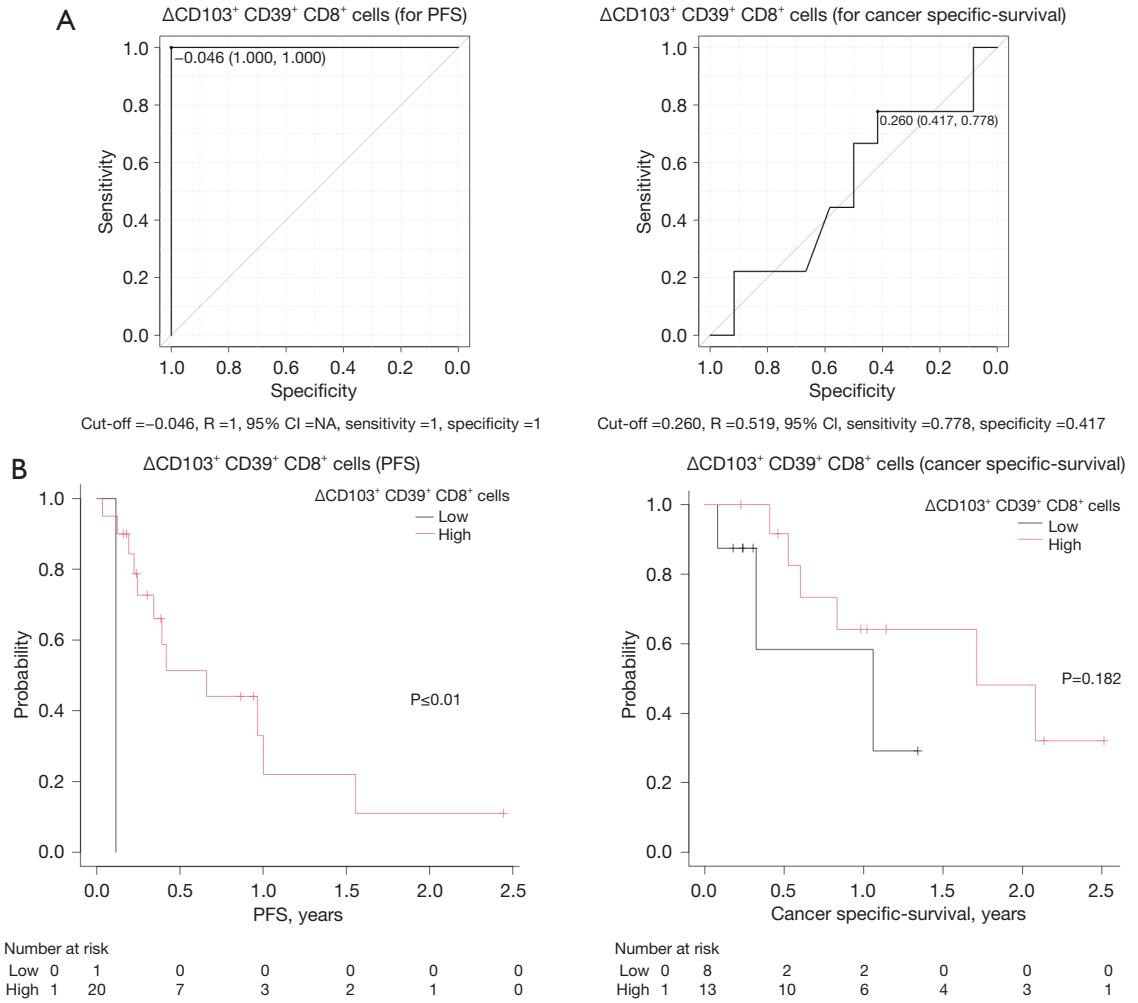

Figure 3 Analysis of the relationship between the increase in CD103$^+$ CD39$^+$ CD8$^+$ cells after ICI and the prognosis was shown. (A) The right and left figures show the ROC curves of the change of CD103$^+$ CD39$^+$ CD8$^+$ cells after the administration of ICI therapy for recurrence and cancer specific-death, respectively. (B) The left and right figures show the Kaplan-Meier curves demonstrating the effects of changes in CD103$^+$ CD39$^+$ CD8$^+$ cells after the administration of ICI therapy for PFS and cancer specific-survival, respectively. PFS, progression-free survival; CI, confidence interval; NA, not available; ICI, immune checkpoint inhibitor; ROC, receiver operating characteristic.

molecules on cancer cells did not affect prognosis, but CD103$^+$ lymphocyte infiltration was reported to be an independently associated with a favorable prognosis (26). It was clarified that CD103$^+$ lymphocytes are involved in the prognosis after surgery. CD103$^+$ TILs have also been reported to be a favorable prognostic factor in various carcinomas (27-30).

Banchereau *et al.* reported that intratumoral CD103$^+$ CD8$^+$ T cells predicted the effect of ICI therapy in lung and bladder cancer patients receiving anti-PD-L1 antibody therapy (31). In addition, although it was a mouse model, it was reported that tumor shrinkage was observed with an increase in the number of CD103$^+$ immune cells in melanoma expressing E-cadherin (32).

Duhen *et al.* reported that in head and neck cancer, CD103$^+$ CD39$^+$ CD8$^+$ T cells killed cancer cells in an MHC class I-restricted manner, and that the prognosis was good if this population was high in intratumorally infiltrating lymphocytes (16). CD39 is an ectonucleotidase that hydrolyzes extracellular adenosine triphosphate and adenosine diphosphate, which is the processed into adenosine, a potent immunoregulator, by CD73 (33).

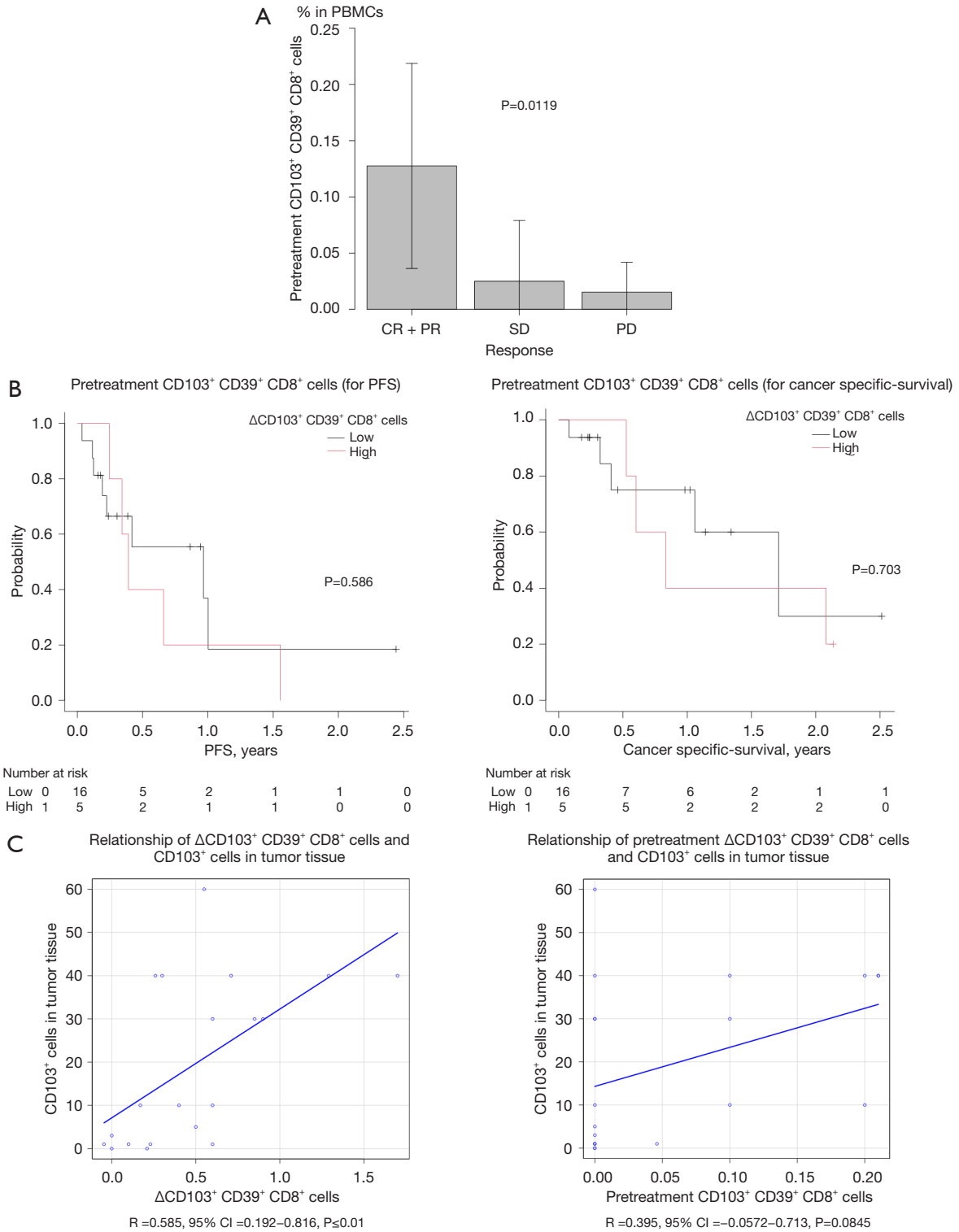

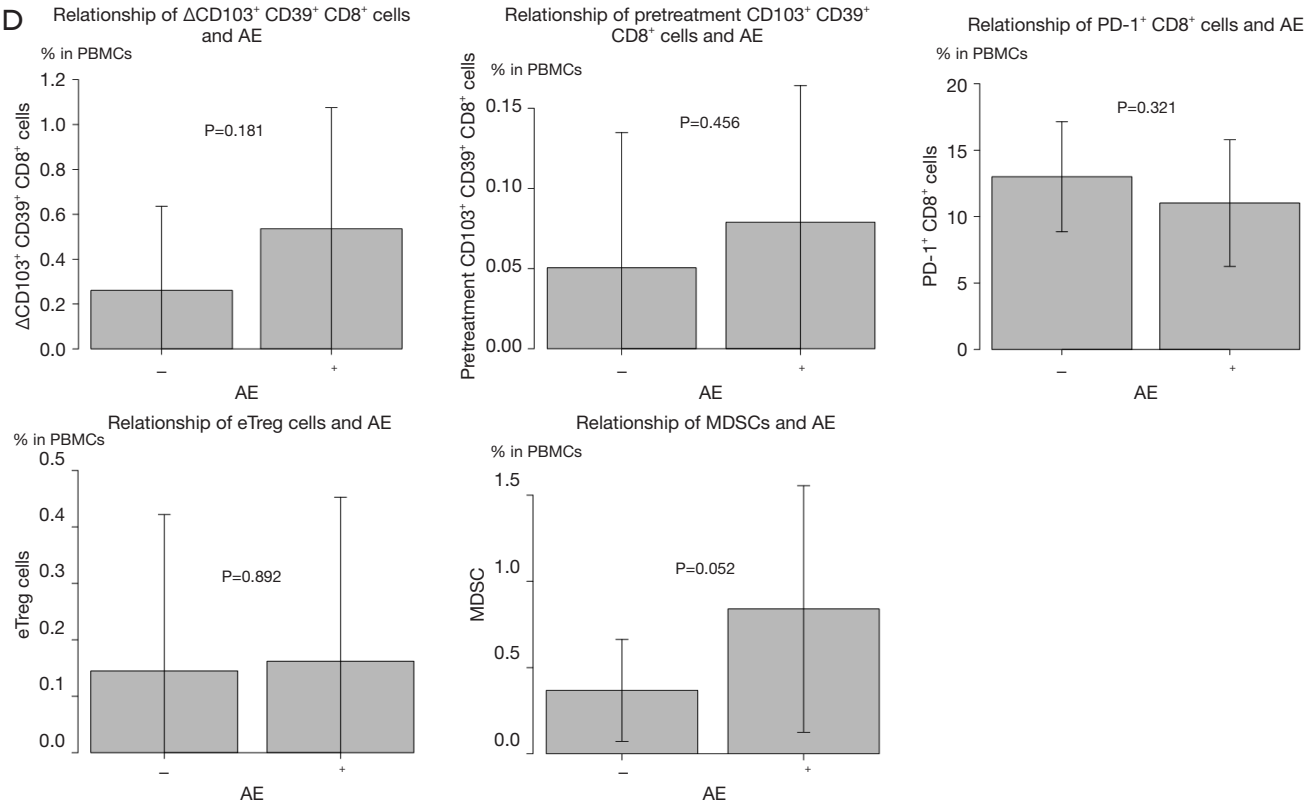

Figure 4 Analysis of the immune molecular profiles of PBMCs and tumor-infiltrating cells was shown. (A) The relationship between CD103$^+$ CD39$^+$ CD8$^+$ cells before the administration of ICI therapy and the clinical response was analyzed by the one-way ANOVA. (B) The left and right figures show Kaplan-Meier curves demonstrating the effects of CD103$^+$ CD39$^+$ CD8$^+$ cells before ICI therapy on PFS and cancer specific-survival, respectively. (C) The right figure shows the analysis of the correlation between intratumor infiltrating CD103$^+$ immune cells before ICI therapy and changes of CD103$^+$ CD39$^+$ CD8$^+$ cells in peripheral PBMCs after the administration of ICI therapy using the Pearson's product-moment correlation coefficient. The left figure shows the correlation between CD103$^+$ immune cells infiltrating the tumor before the administration of ICI therapy and the pretreatment CD103$^+$ CD39$^+$ CD8$^+$ cell count in PBMCs before the administration of ICI therapy. (D) The relationships between typical populations in PBMCs and AEs were analyzed by *t*-test. PBMCs, peripheral blood mononuclear cells; CR, complete response; PR, partial response; SD, stable disease; PD, progressive disease; PFS, progression-free survival; CI, confidence interval; AEs, adverse effects; PD-1, programmed cell death protein-1; eTreg cells, effector regulatory T cells; MDSC, myeloid-derived suppressor cell; ICI, immune checkpoint inhibitor; ANOVA, analysis of variance.

CD103$^+$ CD39$^+$ CD8$^+$ T cells have cancer-specific activity and play a major role in the host's cancer immune response at the forefront.

In this study, in which where the tumor microenvironment contained abundant CD103$^+$ cells before ICI therapy, CD103$^+$ CD39$^+$ CD8$^+$ cells in the blood increased after the administration of ICI. In the first place, CD103$^+$ CD8$^+$ cells are tissue resident memory cells and have a high affinity for tissues, but when they are activated by ICIs and proliferate, they overflow into the peripheral blood. This population has high cancer-specific activity (16) and may be correlated with the positive effects of ICIs. This study is the first report to clarify how changes in CD103$^+$ immune cells in the tumor microenvironment before ICI therapy and CD103$^+$ CD39$^+$ CD8$^+$ cells in PBMCs after ICI therapy influence the effects of ICI therapy. If further cases are accumulated and the observation period is extended, the change in CD103$^+$ CD39$^+$ CD8$^+$ cells in PBMCs after ICI therapy may also be found to have a significant impact on the cancer-specific survival because it was an independent favorable prognostic factor for PFS.

It was reported that the PD-1 expression on CD8$^+$ T cells and Treg cells negatively affects the killing function and immune suppressive function, respectively. Anti PD-1

Table 3 The cut-off value calculated from a ROCs curve

Clinical pathological factor	PFS					Cancer specific-survival				
	Cut-off	R	95% CI	Sensitivity	Specificity	Cut-off	R	95% CI	Sensitivity	Specificity
Age, years	73	0.538	0.248–0.820	0.615	0.625	71	0.639	0.372–0.905	0.667	0.75
Brinkman index	470	0.529	0.263–0.795	0.231	1	1,800	0.519	0.219–0.818	0.33	1
PS	2	0.538	0.335–0.742	0.08	1	1	0.496	0.377–0.614	0.15	0.84
NLR	6.31	0.442	0.177–0.708	0.385	0.75	6.31	0.509	0.236–0.783	0.44	0.75
LDH	226	0.583	0.294–0.873	0.833	0.5	244	0.571	0.3–0.841	1	0.364
CRP	0.61	0.649	0.392–0.906	0.692	0.75	0.59	0.458	0.188–0.729	0.556	0.667
PET SUV	14	0.519	0.175–0.862	0.778	0.5	10	0.562	0.241–0.884	0.625	0.571
Line	1.5	0.452	0.224–0.68	1	0	1.5	0.583	0.367–0.8	0.444	0.75
$CD103^+$ $CD39^+$ $CD8^+$ cells in PBMCs before treatment	0.15	0.683	0.483–0.882	0.385	1	0.15	0.593	0.341–0.845	0.444	0.917
$PD\text{-}1^+$ $CD8^+$ cells in PBMCs before treatment	8.33	0.615	0.346–0.884	0.846	0.5	11.9	0.537	0.27–0.804	0.667	0.5
eTreg cells in PBMCs before treatment	0.14	0.572	0.3–0.844	0.846	0.375	0.12	0.602	0.344–0.859	0.556	0.75
MDSCs in PBMCs before treatment	0.49	0.663	0.416–0.91	0.615	0.875	0.32	0.639	0.373–0.904	0.778	0.667
$\Delta CD103^+$ $CD39^+$ $CD8^+$ cells in PBMCs	−0.046	1	NA–NA	1	1	0.26	0.519	0.252–0.785	0.778	0.417
CD8 by IHC	20	0.552	0.281–0.824	0.75	0.5	10	0.594	0.324–0.864	0.5	0.593
CD103 by IHC	5	0.552	0.278–0.826	0.5	0.75	5	0.562	0.3–0.825	0.5	0.667
MHC class I by IHC	50	0.521	0.23–0.812	0.593	0.625	98	0.536	0.272–0.8	1	0.25
PD-L1 (TCS) by IHC	20	0.672	0.411–0.933	0.75	0.75	20	0.464	0.196–0.731	0.625	0.5
PD-L1 (ICS) by IHC	3	0.573	0.305–0.841	0.583	0.625	3	0.703	0.46–0.946	0.75	0.667

ROC, receiver operating characteristic; PFS, progression-free survival; CI, confidence interval; PS, performance status; NLR, neutrophil-to-lymphocyte ratio; LDH, lactate dehydrogenase; CRP, C-reactive protein; PET, positron emission tomography; SUV, standardized uptake value; PBMC, peripheral blood nuclear cell; PD-1, programmed cell death protein-1; eTreg cells, effector regulatory T cells; MDSC, myeloid-derived suppressor cells; NA, not available; IHC, immunohistochemistry; MHC, major histocompatibility complex; PD-L1, programmed cell death-ligand 1; TCS, tumor cell score; ICS, immune cell score.

therapy induced both the recovery of exhausted $PD\text{-}1^+$ $CD8^+$ T cells and promoted $PD\text{-}1^+$ Treg cell-mediated immune suppression in cancer patients (34). It was also reported that an increase of $PD1^+$ $CD8^+$ T cells in PBMCs after anti-PD-1 antibody therapy was a good prognostic factor in NSCLC patients (35,36). However, $PD\text{-}1^+$ $CD8^+$ T cells were not a significant prognostic factor for ICI in this analysis. No significant difference was detected, even when the analysis was limited to cases in which anti-PD-1 antibodies were administered (data not shown).

Kamada *et al.* reported that anti-PD-1 antibody therapy promoted the suppressive function of Treg cells by promoting the proliferation of eTreg cells in hyperprogressive disease (37). Suzuki *et al.* reported that eTreg cells were highly activated in the tumor microenvironment and suppressed the cellular immune response via immune checkpoint molecules (38). It was also reported that, in breast cancer patients treated

Table 4 Analysis of clinicopathological factors associated with PFS

Clinical pathological factor	Univariate analysis	Multivariate analysis		
	P	HR	95% CI	P
Age, years				
<73	0.562			
≥73				
Sex				
Female	0.43			
Male				
Brinkman index				
<470	0.062	0.1695	0.031–0.937	0.041
≥470				
PS				
<2	0.937			
≥2				
Histology				
Adenocarcinoma	0.103			
Squamous cell carcinoma				
Surgery				
+	0.269			
–				
NLR				
<6.31	0.473			
≥6.31				
LDH				
<226	0.559			
≥226				
CRP				
<0.61	0.767			
≥0.61				
PET SUV				
<14	0.756			
≥14				
Line				
<1.5	0.674			
≥1.5				
$CD103^+$ $CD39^+$ $CD8^+$ cells in PBMCs				
<0.15	0.586			
≥0.15				
PD-1^+ $CD8^+$ cells in PBMCs				
<8.33	0.215			
≥8.33				
eTreg cells in PBMCs				
<0.14	0.593			
≥0.14				
MDSCs in PBMCs				
<0.49	0.483			
≥0.49				
Change of $CD103^+$ $CD39^+$ $CD8^+$ cells in PBMCs				
<0.4	<0.01	0.03894	0.002–0.663	0.025
≥0.4				
CD8 by IHC				
<20	0.336			
≥20				
CD103 by IHC				
<5	0.083	0.3207	0.080–1.283	0.108
≥5				
MHC class I by IHC				
<50	0.967			
≥50				
PD-L1 (TCS) by IHC				
<20	0.32			
≥20				
PD-L1 (ICS) by IHC				
<3	0.959			
≥3				

PFS, progression-free survival; HR, hazard ratio; CI, confidence interval; PS, performance status; NLR, neutrophil-to-lymphocyte ratio; LDH, lactate dehydrogenase; CRP, C-reactive protein; PET, positron emission tomography; SUV, standardized uptake value; PBMC, peripheral blood nuclear cell; PD-1, programmed cell death protein-1; eTreg cells, effector regulatory T cells; MDSC, myeloid-derived suppressor cell; IHC, immunohistochemistry; MHC, major histocompatibility complex; PD-L1, programmed cell death-ligand 1; TCS, tumor cell score; ICS, immune cell score.

Table 5 Analysis of clinicopathological factors associated with cancer-specific survival

Clinical pathological factor	Univariate analysis	Multivariate analysis		
	P	HR	95% CI	P
Age (years)				
<71	0.096	2.308	0.814–1.086	0.401
≥71				
Sex				
Female	0.116			
Male				
Brinkman index				
<1,800	0.008	1.001	0.999–1.002	0.38
≥1,800				
PS				
<1	0.864			
≥1				
Histology				
Adenocarcinoma	0.234			
Squamous cell carcinoma				
Surgery				
+	0.11			
–				
NLR				
<6.31	0.433			
≥6.31				
LDH				
<244	0.434			
≥244				
CRP				
<0.59	0.21			
≥0.59				
PET SUV				
<10	0.936			
≥10				
Line				
<1.5	0.465			
≥1.5				
CD103$^+$ CD39$^+$ CD8$^+$ cells in PBMCs				
<0.15	0.703			
≥0.15				
PD-1$^+$ CD8$^+$ cells in PBMCs				
<8.33	0.086	5.36	0.638–45.180	0.122
≥8.33				
eTreg cells in PBMCs				
<0.14	0.223			
≥0.14				
MDSCs in PBMCs				
<0.49	0.5			
≥0.49				
Change of CD103$^+$ CD39$^+$ CD8$^+$ cells in PBMCs				
<0.26	0.182			
≥0.26				
CD8 by IHC				
<10	0.714			
≥10				
CD103 by IHC				
<5	0.113			
≥5				
MHC class I by IHC				
<98	0.7			
≥98				
PD-L1 (TCS) by IHC				
<20	0.515			
≥20				
PD-L1 (ICS) by IHC				
<3	0.633			
≥3				

HR, hazard ratio; CI, confidence interval; PS, performance status; NLR, neutrophil-to-lymphocyte ratio; LDH, lactate dehydrogenase; CRP, C-reactive protein; PET, positron emission tomography; SUV, standardized uptake value; PBMC, peripheral blood nuclear cell; PD-1, programmed cell death protein-1; eTreg cells, effector regulatory T cells; MDSC, myeloid-derived suppressor cell; IHC, immunohistochemistry; MHC, major histocompatibility complex; PD-L1, programmed cell death-ligand 1; TCS, tumor cell score; ICS, immune cell score.

with anticancer drugs, the prognosis was good in cases where Treg cells and MDSCs in PBMCs decreased after treatment (39). The removal of eTreg cells may lead to enhancement of the effects of ICI therapy, but the pros and cons remain controversial. This analysis did not find any association between the effects of ICIs and AEs and eTreg cells in PBMCs.

MDSCs in humans are defined as $CD11b^+$ $CD14^-$ $CD33^+$ or Lin^- HLA-DR^- $CD33^+$ (40,41). MDSCs can be broadly divided into two subsets. That is, granulocytic MDSCs and monocytic MDSCs. They express the myeloid markers CD11b and CD33, but do not express markers of maturity, such as HLA-DR. We also determined that $CD11b^+$ $CD33^+$ HLA-DR^- cells were MDSCs in this study. Furthermore, granulocytic MDSCs are defined by the expression of CD15, while monocytic MDSCs are defined by the expression of CD14 (42). In the present study, we analyzed the CD11b, CD33, HLA-DR, CD14, and CD15 expression in PBMCs and investigated the relationship between MDSCs and the effect of ICI and AEs, but no significant correlation was detected.

We analyzed the impact of ICI monotherapy on changes in the expression of coinhibitory molecules PD-1, CTLA-4, LAG-3, TIM-3, TIGIT (9), and costimulatory molecules OX40 and 4-1BB (13) of PBMCs; however, the expression levels of these molecules were not significantly associated with the effects of ICI therapy or AEs in this study.

In this study, a high Brinkmann index was independently associated with a favorable prognosis in terms of PFS and was identified as a significant prognostic factor in the univariate analysis of factors associated with cancer-specific survival in this study. The efficacy of ICI therapy in treatment of NSCLC patients varies from individual population to individual population, and the smoking status is also an indicator of the efficacy of ICI therapy (2,4). However, it is hypothesized that the difference in the efficacy of ICI therapy between smokers and nonsmokers is associated with the promotion of gene mutations by smoking; however, the underlying mechanism is unclear. A large number of genes may increase immunogenicity. Sun *et al.* reported that the smoking group had more gene mutations, more copy number polymorphisms, and a stronger immune microenvironment. Smoking is one of the risk factors for carcinogenesis of NSCLC, but it is also a useful predictor of the therapeutic effect of ICIs (43).

In this study, cases were collected and analyzed prospectively; however, the present study was associated with some limitations. Currently, NSCLC patients have less opportunities to receive ICI monotherapy declining; thus, our study population limited as we were only able to enroll 21 cases. There were 12 cases of postoperative recurrence; however, in 4 of these cases, biopsy specimens of the recurrent lesion could not be obtained, and IHC was performed using the primary lesion that was previously resected by surgery. Only 3 cases with anti-PD-L1 antibody administration were included in this analysis, and the results of anti-PD-L1 antibody administration cases were not well reflected. The death rate of 80% is another limitation, if rare populations with a frequency much below 20% are analyzed. Pretreatment $CD103^+$ $CD39^+$ $CD8^+$ T cells correlated with CR and PR, but did not lead to prolongation of PFS and cancer-specific survival. In general, cases with CR and PR often show these prolongations in lung cancer patients treated with ICIs. The reason for this was not well understood from this analysis. It may be necessary to increase the number of cases and analyze to conclude. However, case accumulation has been completed for this analysis, and it is difficult to add further cases. Analysis of the correlation between the change in $CD103^+$ $CD39^+$ $CD8^+$ cells in PBMCs and PFS may have a limitation because there was only one case with fewer than the cut-off for the change in $CD103^+$ $CD39^+$ $CD8^+$ cells in PBMCs. The follow-up period was also limited to the median observation period 220 days.

In this study, the change in $CD103^+$ $CD39^+$ $CD8^+$ cells in PBMCs after the administration of ICI therapy was positively correlated with the effects of ICIs, suggesting that they may be a predictor of the effects of ICI therapy. It was also suggested that in cases in which $CD103^+$ cells infiltrate the tumor microenvironment, ICI therapy may increase the number of $CD103^+$ $CD39^+$ $CD8^+$ cells in the blood.

Acknowledgments

The authors thank Mr. Shinya Yanagi from Department of Diagnostic Pathology, National Hospital Organization, Saitama Hospital for his excellent technical assistance.
Funding: Yoshinobu Ichiki acknowledges grant support from JSPS KAKENHI (Nos. 18K08806, 19K09294, and 22K09013).

Footnote

Reporting Checklist: The authors have completed the REMARK reporting checklist. Available at https://tlcr.amegroups.com/article/view/10.21037/tlcr-22-421/rc

Data Sharing Statement: Available at https://tlcr.amegroups.com/article/view/10.21037/tlcr-22-421/dss

Peer Review File: Available at https://tlcr.amegroups.com/article/view/10.21037/tlcr-22-421/prf

Conflicts of Interest: All authors have completed the ICMJE uniform disclosure form (available at https://tlcr.amegroups.com/article/view/10.21037/tlcr-22-421/coif). The authors have no conflicts of interest to declare.

Ethical Statement: The authors are accountable for all aspects of the work in ensuring that questions related to the accuracy or integrity of any part of the work are appropriately investigated and resolved. This study was conducted in accordance with the Declaration of Helsinki (as revised in 2013). The study protocol was approved by the Saitama Hospital Ethics Committee (No. R2019-02). All participants gave informed consent before participation.

References

1. Brahmer J, Reckamp KL, Baas P, et al. Nivolumab versus Docetaxel in Advanced Squamous-Cell Non-Small-Cell Lung Cancer. N Engl J Med 2015;373:123-35.
2. Borghaei H, Paz-Ares L, Horn L, et al. Nivolumab versus Docetaxel in Advanced Nonsquamous Non-Small-Cell Lung Cancer. N Engl J Med 2015;373:1627-39.
3. Herbst RS, Baas P, Kim DW, et al. Pembrolizumab versus docetaxel for previously treated, PD-L1-positive, advanced non-small-cell lung cancer (KEYNOTE-010): a randomised controlled trial. Lancet 2016;387:1540-50.
4. Reck M, Rodríguez-Abreu D, Robinson AG, et al. Pembrolizumab versus Chemotherapy for PD-L1-Positive Non-Small-Cell Lung Cancer. N Engl J Med 2016;375:1823-33.
5. Brahmer JR, Drake CG, Wollner I, et al. Phase I study of single-agent anti-programmed death-1 (MDX-1106) in refractory solid tumors: safety, clinical activity, pharmacodynamics, and immunologic correlates. J Clin Oncol 2010;28:3167-75.
6. Yu H, Boyle TA, Zhou C, et al. PD-L1 Expression in Lung Cancer. J Thorac Oncol 2016;11:964-75.
7. Wherry EJ, Kurachi M. Molecular and cellular insights into T cell exhaustion. Nat Rev Immunol 2015;15:486-99.
8. Pauken KE, Wherry EJ. Overcoming T cell exhaustion in infection and cancer. Trends Immunol 2015;36:265-76.
9. McLane LM, Abdel-Hakeem MS, Wherry EJ. CD8 T Cell Exhaustion During Chronic Viral Infection and Cancer. Annu Rev Immunol 2019;37:457-95.
10. Callahan MK, Postow MA, Wolchok JD. Targeting T Cell Co-receptors for Cancer Therapy. Immunity 2016;44:1069-78.
11. Huang AC, Postow MA, Orlowski RJ, et al. T-cell invigoration to tumour burden ratio associated with anti-PD-1 response. Nature 2017;545:60-5.
12. Kim KH, Cho J, Ku BM, et al. The First-week Proliferative Response of Peripheral Blood PD-1+CD8+ T Cells Predicts the Response to Anti-PD-1 Therapy in Solid Tumors. Clin Cancer Res 2019;25:2144-54. Erratum in: Clin Cancer Res 2020;26:6610.
13. Croft M. The role of TNF superfamily members in T-cell function and diseases. Nat Rev Immunol 2009;9:271-85.
14. Tanaka A, Sakaguchi S. Regulatory T cells in cancer immunotherapy. Cell Res 2017;27:109-18.
15. Almand B, Clark JI, Nikitina E, et al. Increased production of immature myeloid cells in cancer patients: a mechanism of immunosuppression in cancer. J Immunol 2001;166:678-89.
16. Duhen T, Duhen R, Montler R, et al. Co-expression of CD39 and CD103 identifies tumor-reactive CD8 T cells in human solid tumors. Nat Commun 2018;9:2724.
17. Goldstraw P, Chansky K, Crowley J, et al. The IASLC Lung Cancer Staging Project: Proposals for Revision of the TNM Stage Groupings in the Forthcoming (Eighth) Edition of the TNM Classification for Lung Cancer. J Thorac Oncol 2016;11:39-51.
18. Eisenhauer EA, Therasse P, Bogaerts J, et al. New response evaluation criteria in solid tumours: revised RECIST guideline (version 1.1). Eur J Cancer 2009;45:228-47.
19. Rakaee M, Kilvaer TK, Dalen SM, et al. Evaluation of tumor-infiltrating lymphocytes using routine H&E slides predicts patient survival in resected non-small cell lung cancer. Hum Pathol 2018;79:188-98.
20. Kanda Y. Investigation of the freely available easy-to-use software 'EZR' for medical statistics. Bone Marrow

Transplant 2013;48:452-8.
21. Mueller SN, Mackay LK. Tissue-resident memory T cells: local specialists in immune defence. Nat Rev Immunol 2016;16:79-89.
22. Schenkel JM, Fraser KA, Beura LK, et al. T cell memory. Resident memory CD8 T cells trigger protective innate and adaptive immune responses. Science 2014;346:98-101.
23. Schenkel JM, Masopust D. Tissue-resident memory T cells. Immunity 2014;41:886-97.
24. Fousteri G, Dave A, Juntti T, et al. CD103 is dispensable for anti-viral immunity and autoimmunity in a mouse model of virally-induced autoimmune diabetes. J Autoimmun 2009;32:70-7.
25. El-Asady R, Yuan R, Liu K, et al. TGF-{beta}-dependent CD103 expression by CD8(+) T cells promotes selective destruction of the host intestinal epithelium during graft-versus-host disease. J Exp Med 2005;201:1647-57.
26. Ichiki Y, Ueno M, Yanagi S, et al. An analysis of the immunological tumor microenvironment of primary tumors and regional lymph nodes in squamous cell lung cancer. Transl Lung Cancer Res 2021;10:3520-37.
27. Massi D, Romano E, Rulli E, et al. Baseline β-catenin, programmed death-ligand 1 expression and tumour-infiltrating lymphocytes predict response and poor prognosis in BRAF inhibitor-treated melanoma patients. Eur J Cancer 2017;78:70-81.
28. Wang ZQ, Milne K, Derocher H, et al. CD103 and Intratumoral Immune Response in Breast Cancer. Clin Cancer Res 2016;22:6290-7.
29. Komdeur FL, Wouters MC, Workel HH, et al. CD103+ intraepithelial T cells in high-grade serous ovarian cancer are phenotypically diverse TCRαβ+ CD8αβ+ T cells that can be targeted for cancer immunotherapy. Oncotarget 2016;7:75130-44.
30. Lohneis P, Sinn M, Bischoff S, et al. Cytotoxic tumour-infiltrating T lymphocytes influence outcome in resected pancreatic ductal adenocarcinoma. Eur J Cancer 2017;83:290-301.
31. Banchereau R, Chitre AS, Scherl A, et al. Intratumoral CD103+ CD8+ T cells predict response to PD-L1 blockade. J Immunother Cancer 2021;9:e002231.
32. Shields BD, Koss B, Taylor EM, et al. Loss of E-Cadherin Inhibits CD103 Antitumor Activity and Reduces Checkpoint Blockade Responsiveness in Melanoma. Cancer Res 2019;79:1113-23.
33. Antonioli L, Pacher P, Vizi ES, et al. CD39 and CD73 in immunity and inflammation. Trends Mol Med 2013;19:355-67.
34. Kumagai S, Togashi Y, Kamada T, et al. The PD-1 expression balance between effector and regulatory T cells predicts the clinical efficacy of PD-1 blockade therapies. Nat Immunol 2020;21:1346-58.
35. Kamphorst AO, Pillai RN, Yang S, et al. Proliferation of PD-1+ CD8 T cells in peripheral blood after PD-1-targeted therapy in lung cancer patients. Proc Natl Acad Sci U S A 2017;114:4993-8.
36. Kim CG, Hong MH, Kim KH, et al. Dynamic changes in circulating PD-1+CD8+ T lymphocytes for predicting treatment response to PD-1 blockade in patients with non-small-cell lung cancer. Eur J Cancer 2021;143:113-26.
37. Kamada T, Togashi Y, Tay C, et al. PD-1+ regulatory T cells amplified by PD-1 blockade promote hyperprogression of cancer. Proc Natl Acad Sci U S A 2019;116:9999-10008.
38. Suzuki S, Ogawa T, Sano R, et al. Immune-checkpoint molecules on regulatory T-cells as a potential therapeutic target in head and neck squamous cell cancers. Cancer Sci 2020;111:1943-57.
39. Palazón-Carrión N, Jiménez-Cortegana C, Sánchez-León ML, et al. Circulating immune biomarkers in peripheral blood correlate with clinical outcomes in advanced breast cancer. Sci Rep 2021;11:14426.
40. Zea AH, Rodriguez PC, Atkins MB, et al. Arginase-producing myeloid suppressor cells in renal cell carcinoma patients: a mechanism of tumor evasion. Cancer Res 2005;65:3044-8.
41. Kusmartsev S, Su Z, Heiser A, et al. Reversal of myeloid cell-mediated immunosuppression in patients with metastatic renal cell carcinoma. Clin Cancer Res 2008;14:8270-8.
42. Greten TF, Manns MP, Korangy F. Myeloid derived suppressor cells in human diseases. Int Immunopharmacol 2011;11:802-7.
43. Sun Y, Yang Q, Shen J, et al. The Effect of Smoking on the Immune Microenvironment and Immunogenicity and Its Relationship With the Prognosis of Immune Checkpoint Inhibitors in Non-small Cell Lung Cancer. Front Cell Dev Biol 2021;9:745859.

Cite this article as: Ichiki Y, Fukuyama T, Ueno M, Kanasaki Y, Goto H, Takahashi M, Mikami S, Kobayashi N, Nakanishi K, Hayashi S, Ishida T. Immune profile analysis of peripheral blood and tumors of lung cancer patients treated with immune checkpoint inhibitors. Transl Lung Cancer Res 2022;11(11):2192-2207. doi: 10.21037/tlcr-22-421